• Intelligent Ophthalmology •

Dynamic tear meniscus parameters in complete blinking: insights into dry eye assessment

Ying-Huai Zhang[1,2], *Jun Feng*[3], *Chen-Yuan Yi*[1,2], *Xian-Yu Deng*[1,2], *Yong-Jin Zhou*[1,2], *Lei Tian*[3], *Ying Jie*[3]

[1]Guangdong Key Laboratory of Biomedical Measurements and Ultrasound Imaging, School of Biomedical Engineering, Shenzhen University Medical School, Shenzhen 518060, Guangdong Province, China

[2]Marshall Laboratory of Biomedical Engineering, Shenzhen 518055, Guangdong Province, China

[3]Beijing Ophthalmology and Visual Sciences Key Laboratory, Beijing Tongren Eye Center, Beijing Tongren Hospital, Beijing Institute of Ophthalmology, Capital Medical University, Beijing 100730, China

Co-first authors: Ying-Huai Zhang and Jun Feng
Correspondence to: Yong-Jin Zhou. Guangdong Key Laboratory of Biomedical Measurements and Ultrasound Imaging, School of Biomedical Engineering, Shenzhen University Medical School, Shenzhen 518060, Guangdong Province, China. yjzhou@szu.edu.cn; Lei Tian and Ying Jie. Beijing Institute of Ophthalmology, Beijing Tongren Eye Center, Beijing Tongren Hospital, Capital Medical University, Beijing Ophthalmology and Visual Science Key Lab, No.1 Dong Jiao Min Xiang, Dong Cheng District, Beijing 100730, China. tianlei0131@163.com; jie_yingcn@aliyun.com
Received: 2023-06-10   Accepted: 2023-09-11

Abstract

● **AIM:** To investigate the relationship between dynamic tear meniscus parameters and dry eye using an automated tear meniscus segmentation method.

● **METHODS:** The analysis of tear meniscus videos captured within 5s after a complete blink includes data from 38 participates. By processing video data, several key parameters including the average height of the tear meniscus at different lengths, the curvature of the tear meniscus's upper boundary, and the total area of the tear meniscus in each frame were calculated. The effective values of these dynamic parameters were then linearly fitted to explore the relationship between their changing trends and dry eye disease.

● **RESULTS:** In 94.74% of the samples, the average height of central tear meniscus increased over time. Moreover, 97.37% of the samples exhibited an increase in the overall tear meniscus height (TMH) and area from the nasal to temporal side. Notably, the central TMH increased at a faster rate compared to the nasal side with the temporal side showing the slowest ascent. Statistical analysis indicates that the upper boundary curvature of the whole tear meniscus as well as the tear meniscus of the nasal side (2, 3, and 4 mm) aid in identifying the presence of dry eye and assessing its severity.

● **CONCLUSION:** This study contributes to the understanding of tear meniscus dynamics as potential markers for dry eye, utilizing an automated and non-invasive approach that has implications for clinical assessment.

KEYWORDS: dry eye; dynamic; tear meniscus; blinking
DOI:10.18240/ijo.2023.12.01

INTRODUCTION

D ry eye disease (DED) is a prevalent chronic ocular surface disorder characterized by a loss of tear film homeostasis and the presence of associated ocular surface symptoms. As one of the most common causes for visiting the ophthalmology centers, the prevalence of DED in adults is estimated to be between 5% and 50%[1]. According to the Tear Film & Ocular Surface Society international DED consensus[2], DED can be categorized into two main types based on its underlying pathophysiology mechanisms: aqueous-deficient and evaporative dry eye. Aqueous-deficient DED arises from either insufficient or abnormal secretion of the aqueous component of tear, potentially resulting in an abnormal distribution of tear across the ocular surface[3]. The tear meniscus, constituting approximately 75% to 90%[4] of the total tear volume, plays a pivotal role by supplying the aqueous layer to the tear film following each blink as a part of the ocular surface ecosystem[5-6]. Situated along the margins of the upper and lower eyelids, the tear meniscus height (TMH) is of paramount importance as it reflects tear volume and contributes to the aqueous layer of precorneal tear film[7-9]

Consequently, the measurement of TMH serves as an effective parameter in the diagnosis of DED, particularly in cases of aqueous-deficient DED.

TMH measurement methods can be divided into invasive and non-invasive approaches. The invasive approach employs fluorescein to stain tear meniscus[10]. On the other hand, non-invasive assessments encompass various methodologies such as utilizing a slit lamp with or without reticule, employing kinds of image capture devices, implementing tear interferometry[11], and using optical coherence tomography (OCT)[12-14]. However, these approaches are operator-dependent and tend to exhibit inadequate repeatability, leading to potentially erroneous outcomes. To overcome these limitations, we utilize deep learning techniques as they have excellent repeatability and are a component of artificial intelligence that has been employed in ophthalmic disease diagnosis research[15-17]. Stegmann et al[18] introduced a deep learning segmentation method for the lower tear meniscus based on OCT images. In a similar vein, our research team proposed an automatic segmentation technique for the lower tear meniscus based on deep learning utilizing images captured by the Keratograph 5M Similarly[19]. These approaches demonstrated notable accuracy and effectiveness.

Nevertheless, it should be noted that the values of TMH in the lower tear meniscus undergo temporal change after a blink[20]. Studies have indicated that TMH increases over time following each blink[21-22]. Therefore, the primary aim of this study is to investigate the post-blink variation in TMH and elucidate potential patterns that may reveal sensitive parameters associated with the physiological structure or pathological condition of DED.

SUBJECTS AND METHODS

Ethical Approval The study and data collection were conducted with the approval of the Ethics Committee of Beijing Tongren Hospital (TRECKY2021-238). Informed consent for participation was obtained from all patients and controls.

Subjects The data utilized in this study were collected from Beijing Tongren Hospital and consisted of 27 participants (mean age: 40±12.94y), comprising 3 male and 24 female individuals. A professional ophthalmologist used the Keratograph 5M (K5M; OCULUS Optikgeräte GmbH, Wetzlar, Germany; working at 8 frames/s) to record videos of the lower tear meniscus of both the left and right eyes of each participant, with a duration of approximately 10s per recording[23]. During the recording, participants were instructed to execute a full blink, followed by maintaining their eyes open for as long as possible. Data instances that could not be accurately located or segmented due to image blurriness, participants blinking during the recording, or displacement of the placido disc were excluded. A total of 38 videos were collected from eyes that sustained an open state for more than 5s after a complete blink were collected for this study.

Additionally, the first tear film break-up time (NIBUT.f) and the average tear film break-up time (NIBUT.a) were documented. Based on the NIBUT.f values, DED was diagnosed for each eye of the participants. To investigate the correlation between dynamic parameters of tear meniscus and the presence of DED, the samples were stratified into two groups: DED group (NIBUT.f<10s) and those non-DED group (NIBUT.f≥10s). Similarly, to explore the connection between the meniscus dynamic parameters and the severity of DED, the samples were categorized into three groups: eyes without DED (NIBUT.f≥10s), eyes with mild DED (5s≤NIBUT.f<10s), and eyes with moderate DED (NIBUT.f<5s)[24]. Descriptive statistics for the participants are presented in Table 1.

Parameter Calculation The captured videos were processed into individual frames. The last clear frame indicating closed eyes was designated as the initial frame (frame 0), while the 41st frame, corresponding to a five-second interval after the start frame, was selected as the terminal frame for calculating the dynamic parameters of the tear meniscus for each eye (Figure 1). Subsequently, segmentation was performed on the tear meniscus in each frame, yielding a calculation of seven parameters. These parameters including the overall TMH, TMH values specifically for the central, nasal, and temporal regions, the average upper boundary curvature across the entire tear meniscus, the upper boundary curvature of the central tear meniscus, and the area of the tear meniscus. Additionally, to facilitate a comparative analysis of the impact of different lengths of the tear meniscus within the central, nasal, and temporal regions, this study also calculates these parameters for tear meniscus lengths of 1, 2, 3, 4 mm respectively.

The tear meniscus segmentation model previously proposed by our research team was employed for the purpose of tear meniscus segmentation. Frames with open eyes were input to the network to obtain both the pupil center and the tear meniscus mask. Subsequently, the upper and lower boundaries of the tear meniscus (e_{up} and e_{low}) were subjected to a polynomial fitting process, guided by Formula 1. This fitting procedure was undertaken to achieve a smoother representation of the tear meniscus. The polynomial order, donated as N, was empirically set to 6, a choice made for enhanced performance. The coefficients of the polynomial, represented as w_0, w_1, w_2,..., w_N, played a pivotal role in this fitting process. Furthermore, the calculation of TMH across distinct regions was facilitated using Formula 2. Within this formula, M indicated the pixel-millimeter magnification ratio (86 in this data set) while D denoted the length of the measurement section.
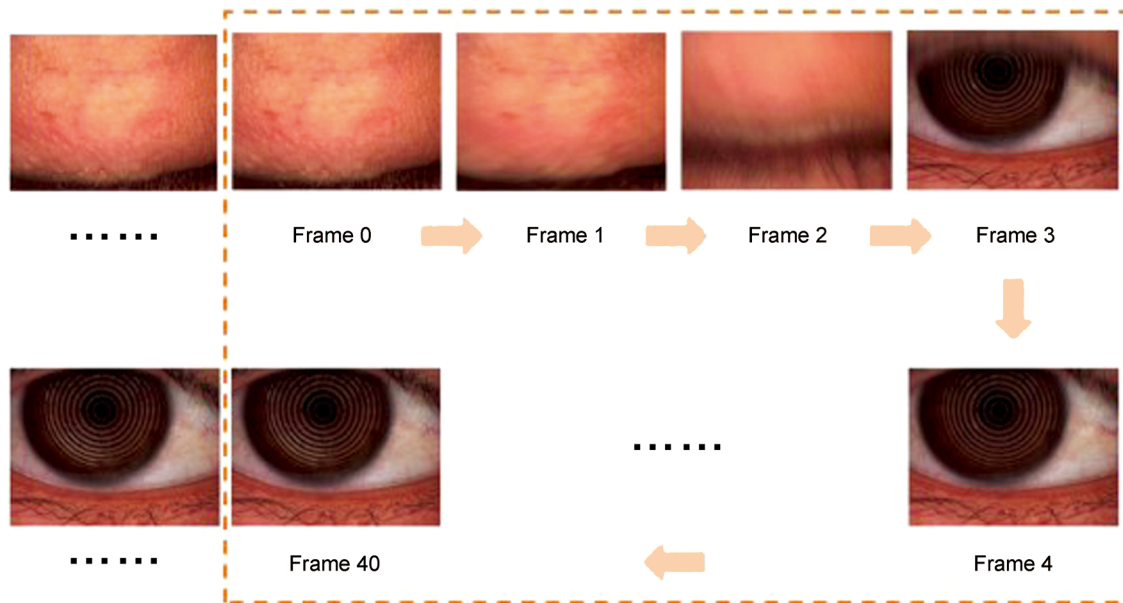
Figure 1 A schematic diagram of image frame selection used to calculate tear meniscus dynamic parameters.

Table 1 Descriptive statistical information of subjects in groups

Parameters	Non-DED group	Mild+moderate DED group	Mild DED group	Moderate DED group
Sample size (n)	5	33	18	15
NIBUT.f (s)	11.13±0.67	5.35±2.27	7.04±1.58	3.32±0.89
NIBUT.a (s)	13.06±0.97	8.47±2.78	9.66±2.10	7.05±2.95

DED: Dry eye disease; NIBUT.f: The first tear film break-up time; NIBUT.a: The average tear film break-up time.

$$z(x,W)=w_0+w_1x+w_2x^2+\cdots+w_Nx^N=\sum_j^N w_jx_j \tag{1}$$

$$TMH=\frac{1}{M}\cdot\frac{|e_{up}-e_{low}|}{D} \tag{2}$$

In addition, Formula 3, where P is the number of pixels of the tear meniscus mask, can be used to calculate the area of the tear meniscus. The curvature of the upper boundary of the tear meniscus in different regions is also calculated using a formula proposed by Zhang et al[25].

$$TM\,Area=\frac{1}{M^2}\cdot P \tag{3}$$

Using the y-axis of the pupil center coordinates as the center, the tear meniscus was sequentially divided into central regions of 1, 2, 3, and 4 mm in length, based on the previous work of our team and a priori knowledge. For left-eye image frames, the leftmost point of the tear meniscus was considered the beginning of the nasal tear meniscus, and the rightmost point was considered the starting point of the temporal tear meniscus. Conversely, for the right-eye images frames, the rightmost point of the tear meniscus was taken as the beginning of the temporal tear meniscus. Different lengths of the nasal and temporal tear meniscus were then selected.

Abnormal image frames that failed to segment the tear meniscus due to movements of the subject's head, eye, or other blurs were assigned a value of 0. We fitted the effective parameters including TMH, curvature, and area of the tear meniscus within the 0–5s using the least squares method, and calculated the slope of the linear fit. Lastly, we performed statistical analysis of the slopes among different DED groups.

Statistical Analysis Statistical analysis for this study was conducted with SPSS 24.0 software (SPSS Inc., Chicago, IL, USA). Because of the small sample size in some groups and the lack of normality in most of the data (as determined by Shapiro-Wilk test), the non-parametric Mann-Whitney test was applied to analyze the differences between participants with and without DED and the slope of the line fitted from the dynamic parameters of the tear meniscus. The Fisher Chi-square test was used to examine the between-group difference analysis between the two groups of samples with or without DED and the two groups of samples with or without positive slopes of their fitted dynamic parameters of the tear meniscus. Welch's ANOVA test was used to analyze the differences among the three participant groups, classified based on having no DED, mild DED, or moderate DED, as well as the slope of the line fitted from dynamic parameters of the tear meniscus. We conducted a Pearson Chi-square test to analyze the between-group difference analysis among three groups of samples, which include normal, mild DED, and moderate DED groups and three groups with or without positive slopes of their fitted dynamic parameters of the tear meniscus. Moreover, we performed a Spearman correlation analysis to assess the relationship between NIBUT and the linear slope of

Table 2 The dynamic parameters of the tear meniscus were calculated for each frame of the sample over a span of 5s

Parameters	k (mean±SD)	No. of k<0	No. of k>0
TMH_middle_1 mm	0.015±0.012	2	36
TMH_nasal_1 mm	0.006±0.018	11	27
TMH_temporal_1 mm	0.011±0.018	6	32
Curve_middle_1 mm	1990.326±9354.557	20	18
TMH_middle_2 mm	0.014±0.011	2	36
TMH_nasal_2 mm	0.008±0.015	8	30
TMH_temporal_2 mm	0.014±0.019	5	33
Curve_middle_2 mm	-153.871±1708.015	18	20
TMH_middle_3 mm	0.014±0.011	2	36
TMH_nasal_3 mm	0.009±0.014	8	30
TMH_temporal_3 mm	0.014±0.017	3	35
Curve_middle_3 mm	52.133±174.861	15	23
TMH_middle_4 mm	0.013±0.010	2	36
TMH_nasal_4 mm	0.009±0.012	8	30
TMH_temporal_4 mm	0.013±0.015	2	36
Curve_middle_4 mm	71.486±421.232	23	15
TMH_all	0.012±0.009	1	37
Curve_all	-275.885±1571.636	23	15
Area	0.207±0.170	1	37

TMH: Tear meniscus height.

Figure 2 The visualization result of the segmentation of the tear meniscus The green origin represents the pupil center. The green dashed line represents the y-axis, which is the central axis of the central tear meniscus. The leftmost green and red solid lines show the upper and lower boundaries of the segmented left tear meniscus. The middle blue and orange solid lines display the upper and lower boundaries of the central tear meniscus. The right purple and pink lines indicate the upper and lower boundaries of the right tear meniscus. The TMH between the left, central and right tear meniscus are shown inside the black box located the upper left corner. TMH: Tear meniscus height.

the dynamic parameters fitted to the tear meniscus. A *P*-value below 0.05 was considered statistically significant.

RESULTS

Figure 2 visually confirms the correct segmentation of the tear meniscus by visualizing the boundaries of the tear meniscus, along with the average TMH in the left, right, and central regions of each frame. Figure 3 presents line graphs were depicting the 7 dynamic parameters of the tear meniscus calculated for each frame and the time variation. In addition, the trend lines obtained by linear fitting to the parameters are plotted.

Table 2 depicts the results of the descriptive statistical analysis of the trend straight-line slope obtained by fitting the seven dynamic parameters of the tear meniscus calculated for the 38 case samples. It can be inferred that the TMH of most subjects' eyes increased to varying degrees within 5s after blinking. This increase was observed both in the partial tear meniscus of different lengths and in the whole tear meniscus, particularly in the TMH of the central region and the overall TMH. In addition, among the tear meniscus of different lengths, the slope of the trend straight line obtained by fitting the TMH of the central region was always greater than or equal to that of the TMH of the nasal side. The TMH of the temporal side, on the slowest average rising trend.

To investigate whether the trend in the dynamic parameter of tear meniscus obtained from the above calculation correlated with the DED, we performed an analysis of the differences
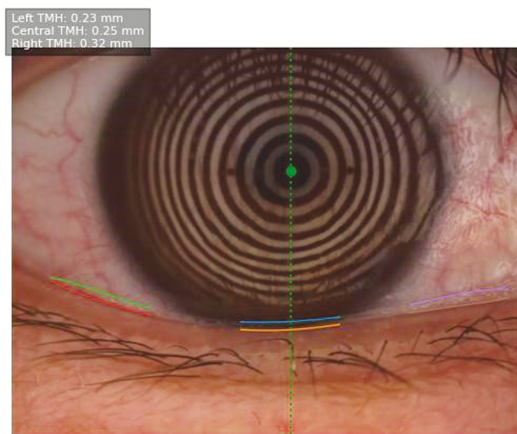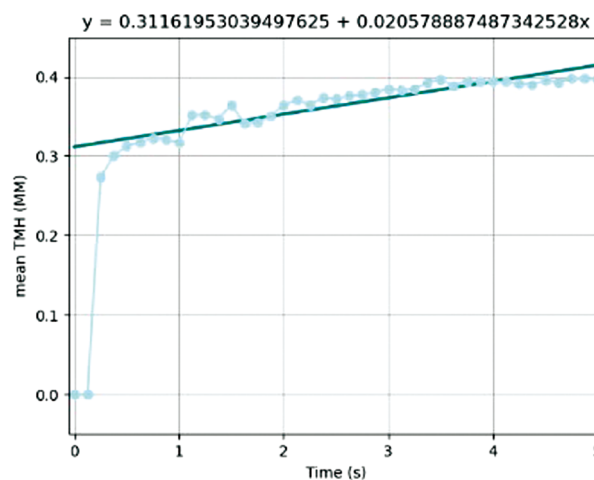

Figure 3 Trend plots of the dynamic parameters of the tear meniscus over the period of 0 to 5s The light blue dashes represent the dynamic parameter of the tear meniscus at each moment and the dark blue-green line shows the trend lines that were obtained by linearly fitting the effective parameters. TMH served as an example in this figure. TMH: Tear meniscus height.

between groups for each of the two groups of subject eyes classified as having or not DED according to NIBUT.f (Table 3), and for each of the three groups classified as without DED group, the DED group, the mild DED group and the moderate DED group (Table 4). The results showed that the slope of the straight line fitted to the upper border curvature of the whole tear meniscus was significantly different between the groups with and without DED (*P*=0.024). In the three groups

Table 3 The results of the between-group difference analysis of the dynamic parameters

Parameters	DED	Non-DED	U	P
TMH_middle_1 mm	0.011 (0.007, 0.041)	0.138 (0.006, 0.021)	64	0.449
TMH_nasal_1 mm	-0.006 (-0.014, 0.011)	0.005 (0.000, 0.016)	46	0.123
TMH_temporal_1 mm	0.023 (0.002, 0.050)	0.007 (0.002, 0.019)	46	0.123
Curve_middle_1 mm	32.661 (-50.602, 88.333)	-57.054 (-345.802, 400.978)	72	0.675
TMH_middle_2 mm	0.011 (0.004, 0.040)	0.125 (0.005, 0.021)	70	0.615
TMH_nasal_2 mm	-0.008 (-0.015, 0.012)	0.010 (0.002, 0.017)	41	0.076
TMH_temporal_2 mm	0.031 (0.004, 0.056)	0.011 (0.004, 0.020)	45	0.112
Curve_middle_2 mm	-31.860 (-164.977, 263.968)	2.109 (-278.131, 209.321)	81	0.967
TMH_middle_3 mm	0.011 (0.005, 0.039)	0.143 (0.005, 0.021)	73	0.706
TMH_nasal_3 mm	-0.002 (-0.013, 0.012)	0.010 (0.003, 0.018)	40	0.069
TMH_temporal_3 mm	0.030 (0.005, 0.052)	0.010 (0.003, 0.021)	50	0.172
Curve_middle_3 mm	29.823 (-33.765, 113.391)	16.017 (-27.596, 57.918)	78	0.867
TMH_middle_4 mm	0.011 (0.005, 0.037)	0.012 (0.005, 0.020)	71	0.645
TMH_nasal_4 mm	-0.002 (0.005, 0.045)	0.010 (0.002, 0.016)	48	0.146
TMH_temporal_4 mm	0.028 (0.005, 0.045)	0.009 (0.004, 0.020)	51	0.187
Curve_middle_4 mm	140.195 (-27.993, 465.989)	-22.621 (-66.532, 14.609)	42	0.084
TMH_all	0.014 (0.002, 0.027)	0.012 (0.005, 0.157)	78	0.867
Curve_all	19.122 (5.597, 58.670)	-10.134 (-32.643, 12.072)	31	0.024
Area	0.220 (0.077, 0.353)	0.187 (0.101, 0.247)	79	0.900

Mann-Whitney test was used. DED: Dry eye disease; TMH: Tear meniscus height.

Table 4 The results of the between-group analysis of the dynamic parameters

Parameters	DED	Mild DED	Moderate DED	P
TMH_middle_1 mm	0.022±0.020	0.015±0.012	0.013±0.010	0.397
TMH_nasal_1 mm	-0.002±0.018	0.011±0.015	0.003±0.020	0.233
TMH_temporal_1 mm	0.025±0.028	0.010±0.011	0.009±0.021	0.202
Curve_middle_1 mm	21.624±78.548	2188.473±9948.341	2408.783±10757.31	0.887
TMH_middle_2 mm	0.020±0.021	0.013±0.008	0.012±0.009	0.385
TMH_nasal_2 mm	-0.003±0.016	0.011±0.014	0.007±0.016	0.222
TMH_temporal_2 mm	0.030±0.029	0.012±0.010	0.011±0.022	0.121
Curve_middle_2 mm	33.224±243.585	560.006±1888.453	271.126±1775.647	0.387
TMH_middle_3 mm	0.014±0.009	0.020±0.019	0.010±0.014	0.205
TMH_nasal_3 mm	-0.001±0.014	0.012±0.014	0.010±0.014	0.205
TMH_temporal_3 mm	0.029±0.026	0.011±0.009	0.012±0.021	0.129
Curve_middle_3 mm	37.815±82.895	77.278±246.412	26.732±75.644	0.715
TMH_middle_4 mm	0.019±0.019	0.013±0.008	0.012±0.0029	0.427
TMH_nasal_4 mm	0.000±0.012	0.011±0.013	0.009±0.012	0.275
TMH_temporal_4 mm	0.026±0.023	0.011±0.008	0.012±0.018	0.152
Curve_middle_4 mm	203.238±281.941	124.112±590.894	-35.583±113.511	0.044
TMH_all	0.015±0.014	0.012±0.007	0.011±0.011	0.828
Curve_all	29.531±28.532	546.055±2308.831	-53.487±225.859	0.621
Area	0.216±0.150	0.234±0.174	0.172±0.182	0.597

Welch's ANOVA test was used. DED: Dry eye disease; TMH: Tear meniscus height.

classified according to the degree of DED, the slope of the line fitted to the central tear meniscus of length 4 mm also displayed a significant difference between the groups with and without DED (P=0.044).

We classified the slope k of the fitted straight lines for the dynamic parameters calculated above into positive and negative groups and performed Chi-square tests among them. One group consisted of subjects with DED, whereas the other group included subjects without DED. Additionally, we also conducted Chi-square tests among three groups of subjects classified according to the prevalence degree of DED. The results of the tests are demonstrated in Tables 5 and 6.

Table 5 The results of the between-group difference analysis of the slope

Slope	Non-DED group	DED group
TMH_middle_1 mm, *n*		
Positive	5	30
Negative	0	3
P		1.000
TMH_nasal_1 mm, *n*		
Positive	2	25
Negative	3	8
P		0.1342
TMH_temporal_1 mm, *n*		
Positive	7	28
Negative	1	5
P		1.0002
Curve_middle_1 mm, *n*		
Positive	3	15
Negative	2	18
P		0.6532
TMH_middle_2 mm, *n*		
Positive	5	30
Negative	0	3
P		1.0002
TMH_nasal_2 mm, *n*		
Positive	2	28
Negative	3	5
P		0.0532
TMH_temporal_2 mm, *n*		
Positive	4	30
Negative	1	3
P		0.4462
Curve_middle_2 mm, *n*		
Positive	2	18
Negative	3	15
P		0.6532
TMH_middle_3 mm, *n*		
Positive	5	31
Negative	0	2
P		1.000
TMH_nasal_3 mm, *n*		
Positive	2	28
Negative	3	5
P		0.0532
TMH_temporal_3 mm, *n*		
Positive	4	31
Negative	1	2
P		0.3532
Curve_middle_3 mm, *n*		
Positive	3	20
Negative	2	13
P		1.0002
TMH_middle_4 mm, *n*	5	31
Positive	0	2
Negative		1.0002
P		
TMH_nasal_4 mm, *n*		
Positive	2	28
Negative	3	5
P		0.053
TMH_temporal_4 mm, *n*		
Positive	4	32
Negative	1	1
P		0.2492
Curve_middle_4 mm, *n*		
Positive	3	12
Negative	2	21
P		0.3652
TMH_all, *n*		
Positive	5	32
Negative	0	1
P		1.0002
Curve_all, *n*		
Positive	4	11
Negative	1	22
P		0.0692
Area, *n*		
Positive	5	32
Negative	0	1
P		1.0002

Fisher Chi-square test was used. DED: Dry eye disease; TMH: Tear meniscus height.

Based on the results, we concluded that were no significant differences observed in the positive and negative k values fitted to the dynamic parameters, between the two groups of subjects with and without DED. In contrast, in all three groups of data classified according to the degree of DED prevalence, significant differences were observed in the nasal side of the TMH with lengths of 2, 3, and 4 mm, respectively (*P*=0.024).

DISCUSSION

This study is founded on the automated TMH segmentation method proposed by our team. We calculated several key parameters by processing video data collected within five seconds following a full blink from 38 subjects. The parameters we computed consisted of the average TMH at different lengths, the curvature of the upper boundary of the tear meniscus, and the total area of the tear meniscus in each frame. The effective values of these dynamic parameters were then linearly fitted to explore the relationship between their changing trends and DED.

Among all 38 samples, our analysis indicates that 36 cases (94.74%) demonstrated an increasing trend in the average height of the central tear meniscus and 37 cases (97.37%) indicated a growing trend in the overall average height and area of the tear meniscus from the nasal to the temporal side over time. It is noteworthy that the TMH in most of the designated nasal and temporal areas also displayed an increase over time. This result further confirms the previous conclusion that the TMH tends to increases after a complete blink.

In addition, observed a correlation where increasing length of the tear meniscus being observed coincided with an increased number of samples demonstrating an upward trend in the TMH

Table 6 The results of the between-group difference analysis of the slope

Slope	Non-DED group	Mild DED group	Moderate DED group
TMH_middle_1 mm, *n*			
Positive	5	18	12
Negative	0	0	3
P		0.082	
TMH_nasal_1 mm, *n*			
Positive	2	14	11
Negative	3	4	4
P		0.249	
TMH_temporal_1 mm, *n*			
Positive	4	17	11
Negative	1	1	4
P		0.2442	
Curve_middle_1 mm, *n*			
Positive	3	7	8
Negative	2	11	7
P		0.5912	
TMH_middle_2 mm, *n*			
Positive	5	18	12
Negative	0	0	3
P		0.082	
TMH_nasal_2 mm, *n*			
Positive	2	17	11
Negative	3	1	4
P		0.024	
TMH_temporal_2 mm, *n*			
Positive	4	17	13
Negative	1	1	2
P		0.584	
Curve_middle_2 mm, *n*			
Positive	2	10	8
Negative	3	8	7
P		0.825	
TMH_middle_3 mm, *n*			
Positive	5	18	13
Negative	0	0	2
P		0.198	
TMH_nasal_3 mm, *n*			
Positive	2	17	11
Negative	3	1	4
P		0.0242	
TMH_temporal_3 mm, *n*			
Positive	4	17	14
Negative	1	1	1
P		0.9982	
Curve_middle_3 mm, *n*			
Positive	3	11	9
Negative	2	7	6
P		0.9982	
TMH_middle_4 mm, *n*			
Positive	5	18	13
Negative	0	0	2
P		0.1982	
TMH_nasal_4 mm, *n*			
Positive	2	17	11
Negative	3	1	4
P		0.0242	
TMH_temporal_4 mm, *n*			
Positive	4	18	14
Negative	1	0	1
P		0.1982	
Curve_middle_4 mm, *n*			
Positive	3	8	4
Negative	2	10	11
P		0.3502	
TMH_all, *n*			
Positive	5	18	14
Negative	0	0	1
P		0.4552	
Curve_all			
Positive	4	5	6
Negative	1	13	9
P		0.1072	
Area, *n*			
Positive	5	18	14
Negative	0	0	1
P		0.4552	

Pearson Chi-Square test was used. DED: Dry eye disease; TMH: Tear meniscus height.

on the nasal and temporal sides. Notably, during the dynamic changes of TMH, it appeared that the central average TMH grew at a faster pace or at the same rate as the nasal TMH, while the temporal TMH showed the slowest increasing trend.

The statistical results suggest that changes in the curvature of the upper boundary curvature of the entire tear meniscus during the first 5s after a full blink may be related to the presence of DED. Moreover, the trends of the TMH of the nasal side in 2, 3, and 4 mm during the same five-second period may assist in identifying the severity of DED in our collected data.

To summarize, our research indicates that there are dynamic changes in TMH following a blink. It is possible that the physiological structure of the eye and/or the presence of DED correlate with these changes. This observation is consistent with previous research that has shown that after a blink, TMH increases over time[10-11].

However, it is crucial to acknowledge that while this study substantiates the dynamic changes in TMH after blinking, it has certain limitations. Firstly, the videos collected in this study were captured with K5M equipment, which can only show the dynamic changes in the flat tear meniscus, making it difficult to accurately quantify the changes in tear volume. Additionally, discomfort from DED may cause some subjects to blink incompletely during testing, which can lead to blurry tear meniscus and sudden decreases in height, which may impact the study's results. Lastly, the study only included 5 samples of the subjects' eyes without DED, while the remaining 33 samples had varying degrees of DED. Therefore, future research should aim to obtain a more balanced sample distribution.

In conclusion, based on our study, we have confirmed that TMH undergoes dynamic changes after a complete blink. Moreover, we have identified several parameters that are sensitive to the physiological structure or pathological state of DED.

Our findings demonstrate that the most of our sample (94.74%) experienced an upward trend in the average height of the central tear meniscus as well as the overall TMH and area in the nasal-temporal direction after a blink. We also observed a higher count of samples with a trend of increasing average TMH in both the nasal and temporal areas as the length of tear meniscus increase. This study provides new insights into the dynamic changes in TMH after a blink. Identifying of diagnostic parameters based on these changes could potentially have significant clinical implications for the diagnosis and management of DED.

ACKNOWLEDGEMENTS

REFERENCES

1 Stapleton F, Garrett Q, Chan C, Craig JP. *The epidemiology of dry eye disease*. Dry Eye. Berlin, Heidelberg: Springer Berlin Heidelberg, 2014:21-29.

2 Craig JP, Nichols KK, Akpek EK, *et al*. TFOS DEWS II definition and classification report. *Ocul Surf* 2017;15(3):276-283.

3 Bron AJ, de Paiva CS, Chauhan SK, *et al*. TFOS DEWS II pathophysiology report. *Ocul Surf* 2017;15(3):438-510.

4 Niedernolte B, Trunk L, Wolffsohn JS, Pult H, Bandlitz S. Evaluation of tear meniscus height using different clinical methods. *Clin Exp Optom* 2021;104(5):583-588.

5 Wan C, Hua RR, Guo P, Lin PJ, Wang JT, Yang WH, Hong XQ. Measurement method of tear meniscus height based on deep learning. *Front Med* (*Lausanne*) 2023;10:1126754.

6 Rao SK, Gokhale N, Matalia H, Mehta P. Inflammation and dry eye disease—where are we? *Int J Ophthalmol* 2022;15(5):820-827.

7 Sang X, Li Y, Yang L, *et al*. Lipid layer thickness and tear meniscus height measurements for the differential diagnosis of evaporative dry eye subtypes. *Int J Ophthalmol* 2018;11(9):1496-1502.

8 Wolffsohn JS, Arita R, Chalmers R, *et al*. TFOS DEWS II diagnostic methodology report. *Ocular Surf* 2017;15(3):539-574.

9 Tung CI, Perin AF, Gumus K, Pflugfelder SC. Tear meniscus dimensions in tear dysfunction and their correlation with clinical parameters. *Am J Ophthalmol* 2014;157(2):301-310.e1.

10 Wu ZW, Begley CG, Port N, Bradley A, Braun R, King-Smith E. The effects of increasing ocular surface stimulation on blinking and tear secretion. *Invest Ophthalmol Vis Sci* 2015;56(8):4211.

11 Arita R, Yabusaki K, Hirono T, Yamauchi T, Ichihashi T, Fukuoka S, Morishige N. Automated measurement of tear meniscus height with the kowa DR-1α tear interferometer in both healthy subjects and dry eye patients. *Invest Ophthalmol Vis Sci* 2019;60(6):2092-2101.

12 Yuan YM, Wang JH, Chen Q, Tao AZ, Shen MX, Shousha MA. Reduced tear meniscus dynamics in dry eye patients with aqueous tear deficiency. *Am J Ophthalmol* 2010;149(6):932-938.e1.

13 Czajkowski G, Kaluzny BJ, Laudencka A, Malukiewicz G, Kaluzny JJ. Tear meniscus measurement by spectral optical coherence tomography. *Optom Vis Sci* 2012;89(3):336-342.

14 Wang J. Relationships between central tear film thickness and tear menisci of the upper and lower eyelids. *Invest Ophthalmol Vis Sci* 2006;47(10):4349-4355.

15 Kapoor R, Walters SP, Al-Aswad LA. The Current state of artificial intelligence in ophthalmology. *Surv Ophthalmol* 2019;64(2):233-240.

16 Yang WH, Shao Y, Xu YW, Ophthalmic Imaging and Intelligent Medicine Branch of Chinese Medicine Education Association Expert Workgroup of Guidelines on Clinical Research Evaluation of Artificial Intelligence in Ophthalmology (2023). Guidelines on clinical research evaluation of artificial intelligence in ophthalmology (2023). *Int J Ophthalmol* 2023;16(9):1361-1372.

17 Zhao JQ, Lu Y, Zhu SJ, Li KR, Jiang Q, Yang WH. Systematic bibliometric and visualized analysis of research hotspots and trends on the application of artificial intelligence in ophthalmic disease diagnosis. *Front Pharmacol* 2022;13:930520.

18 Stegmann H, Werkmeister RM, Pfister M, Garhöfer G, Schmetterer L, Dos Santos VA. Deep learning segmentation for optical coherence tomography measurements of the lower tear meniscus. *Biomed Opt Express* 2020;11(3):1539-1554.

19 Deng XY, Tian L, Liu ZY, Zhou YJ, Jie Y. A deep learning approach for the quantification of lower tear meniscus height. *Biomed Signal Process Control* 2021;68:102655.

20 Shen MX, Wang JH, Tao AZ, Chen Q, Lin SC, Qu J, Lu F. Diurnal variation of upper and lower tear menisci. *Am J Ophthalmol* 2008;145(5):801-806.e2.

21 Johnson ME, Murphy PJ. Temporal changes in the tear menisci following a blink. *Exp Eye Res* 2006;83(3):517-525.

22 Palakuru JR, Wang JH, Aquavella JV. Effect of blinking on tear dynamics. *Invest Ophthalmol Vis Sci* 2007;48(7):3032.

23 Wei AJ, Le QH, Hong JX, Wang WT, Wang F, Xu JJ. Assessment of lower tear meniscus. *Optom Vis Sci* 2016;93(11):1420-1425.

24 The definition and classification of dry eye disease: report of the definition and classification subcommittee of the international dry eye workshop (2007). *Ocular Surf* 2007;5(2):75-92.

25 Zhang PJ, Wang CB, Ye L. A type III radio burst automatic analysis system and statistic results for a half solar cycle with Nançay Decameter Array data. *Astron Astrophys* 2018;618:A165.